Case Studies in Engineering Failure Analysis 2 (2014) 91–99

Contents lists available at ScienceDirect

Case Studies in Engineering Failure Analysis

journal homepage: www.elsevier.com/locate/csefa

In vivo shell-like fractures of veneered-ZrO_2 fixed dental prostheses

Renan Belli [a], Susanne S. Scherrer [b], Sven Reich [c], Anselm Petschelt [a], Ulrich Lohbauer [a,*]

[a] *Laboratory for Biomaterials Research, Dental Clinic 1 – Operative Dentistry and Periodontology, Friedrich-Alexander University of Erlangen-Nuremberg, Glueckstrasse 11, D-91054 Erlangen, Germany*
[b] *Department of Prosthodontics-Biomaterials, School of Dental Medicine, University of Geneva, Switzerland*
[c] *Department of Prosthodontics and Biomaterials, Center of Implantology, Medical Faculty, RWTH Aachen University, Pauwelsstraße 30, 52074 Aachen, Germany*

ARTICLE INFO

Article history:
Received 24 March 2014
Received in revised form 4 June 2014
Accepted 5 June 2014
Available online 12 June 2014

Keywords:
Dental fractography
Dental ceramics
Dental prosthesis
Zirconia
Glass–ceramic
Contact damage

ABSTRACT

Fractographic analyses are performed in two fixed dental prosthetic reconstructions made of ZrO_2 frameworks covered by a veneering ceramic that fractured during function in the mouth. Processing histories, material properties, recovered broken parts and replicas of the fracture surface were used, along with fractographic markings to determine fracture origins and cause of failure. A shell-like fracture pattern was found common for both cases, although different factors were identified to be involved in each fracture event. Internal thermal residual stresses and occlusal surface defects from localized contact overloading were found to precipitate the fracture in Case 1, whereas extreme occlusal surface damage from sliding chewing contact was determinant in the fracture of Case 2. The interface between the veneering ceramic and the ZrO_2 framework was unaffected by the fractures.

1. Introduction

Until the end of the last century most fixed dental prosthetic reconstructions were based on metal alloys, which could be sinter-covered with a veneering ceramic (usually a silicate glass reinforced with feldspar, leucite or other crystals). That scenario changed with the ingress of glass-infiltrated alumina ceramics in the late 90s for use as framework, and later with the possibility to machine these out of green bodies of zirconium dioxide (ZrO_2), alumina-ZrO_2-glass composites or pure alumina. Due to the reputation of ZrO_2 as a high-toughness high-strength ceramic, it absorbs today a large fraction of treatment demands requiring short- and long-span structural reinforcement, with high clinical success rates regarding frameworks [1].

The down side to ZrO_2-based dental constructs was first recognized in 2006–2007, when results from the earliest clinical trials reported on the high fracture incidences of the overlying veneering ceramic after only a few months in service [2,3]. The numbers were high compared to conventional metal–ceramic systems [4], with more severe clinical consequences often

* Corresponding author. Tel.: +49 9131 854 3740; fax: +49 9131 853 4207.
E-mail addresses: ulrich.lohbauer@fau.de, lohbauer@dent.uni-erlangen.de (U. Lohbauer).

http://dx.doi.org/10.1016/j.csefa.2014.06.001

leading to complete restoration replacement [5]. Thorough fractographic analysis of dental ceramic fracture cases are rare [5–9], and for zirconia almost inexistent [5].

First speculations implicated the quality of the interface between the framework and the veneering material. Today, the current scientific opinion supports the theory that thermal-induced residual stresses are responsible for the acceleration of fracture in veneered-ZrO_2 prostheses. Such stresses also develop in metal–ceramic structures, for which bench-cooling protocols were made routine in order to put the veneering material under compression. Inadvertently, laboratories kept the same practice for all-ceramic systems, disregarding the low thermal conductivity of ceramic materials and its implications. Thereby, temperature differences during cooling can reach 100–140 °C within the veneer thickness when ZrO_2 is used as the substrate, in contrast to 20–90 °C for metal–ceramic systems [6]. A residual stress gradient then develops during solidification due to the inability of the glass to relax at the pace of the rapid cooling rate. To minimize residual stress build-up, current recommendations advocate slow-cooling protocols and the use of veneering materials with matching

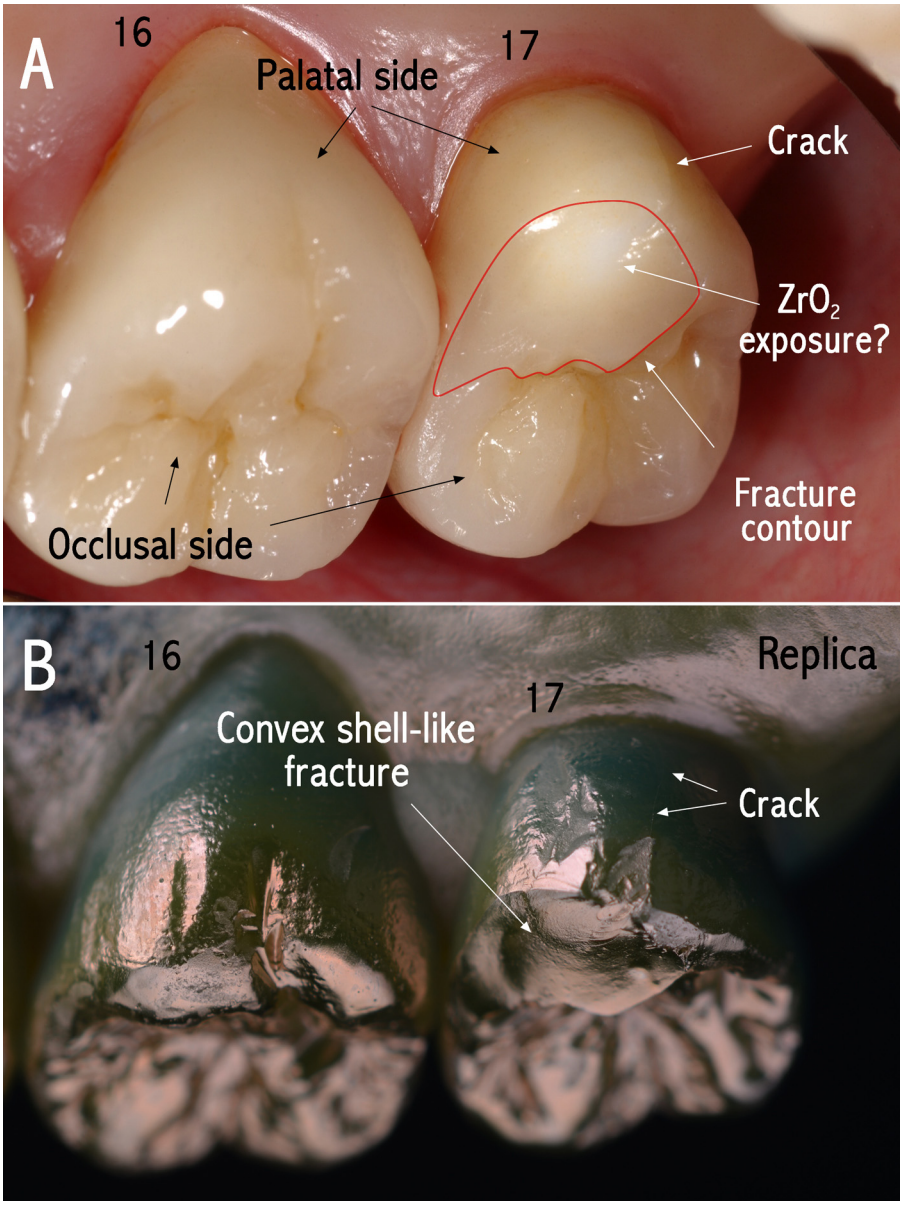

Fig. 1. (A) Palatal view of the clinical situation of Case 1. A fracture of the veneer material of the veneer-ZrO_2 crown of element 17 is outlined in red. A whitish area on the fracture surface indicates that the underlying ZrO_2 framework might have been exposed. A crack can be seen running through the palatal surface connecting the to the cervical margin of the crown. (B) Palatal view of the gold-sputtered replica from an *in situ* impression (A). With a lateral illumination reflections allow for the convex fracture surface to be distinguished. A crack (A) can be seen running from broken surface and connecting with the palatal (cervical) margin. Images (A) and (B) are oriented as in reality, following the position of teeth in the upper arch. The following SEM images are presented in particular orientations for a better understanding of the fractographic analysis.

coefficients of thermal expansion (CTE) to the ZrO_2 framework. Unfortunately, dental ceramic manufacturers were slow in adjusting the CTEs of their products, which derived from the ones used for veneering metals. Today the market still offers material combinations presenting CTE mismatches as high as 2 ppm/°C.

The purpose of this research paper is to describe two veneering ceramic fractures over ZrO_2 framework dental prostheses, which resulted in convex fracture surfaces and shell-like veneer fragments. Background data was gathered regarding material specifications and processing histories. Full fractographic analyses were performed in retrieved fragments and/or replicas taken *in situ* in order to determine the fracture origins and possible causes of failure.

2. Background

2.1. Case 1: single crown

The clinical appearance of the first case is shown in Fig. 1a. Both shown elements are single veneered-ZrO_2 crowns from the first and second upper right molars (FDI numbering system: #16, #17). In crown #17, the fracture of the veneering ceramic can be observed involving the palatal cusp and extending towards the approximal mesial ridge. The fragment was not recovered. A crack is visible emanating from the palatal periphery of the fracture surface and running towards the cervical margin. On the fractured surface the whitish appearance is the underlying zirconia framework, but SEM is needed to determine if zirconia is exposed. The convexity of the fracture surface is better seen from the optical images of the gold-sputtered replica (Fig. 1b).

Information received from the dentist dates the installation of the prosthetic work to February 13, 2007, approx. 32 months before the fracture event (October 20, 2009). The ceramic crown had been luted to the abutment tooth with a glass-ionomer cement (Ketac Cem, 3M ESPE, Seefeld, Germany), and the antagonist element consisted of an implant-supported all-ceramic single crown, which had been in service during the whole period. Consultation of the manufacturing laboratory archives revealed that the core material was a ZrO_2 (Yttria-stabilized Tetragonal Zirconia Polycrystals, 3Y-TZP) machined in a presintered state from a Kavo ZS Disc (Kavo, Biberach, Germany) having a CTE of 10.5 ppm/°C. The veneering ceramic was leucite-based (Creation Zi-CT, Willi Geller, Meiningen, Austria) having a CTE of 8.6 ppm/°C, and applied using the layering technique. The furnace used to sinter the veneering ceramic was an Austromat 3001 (Dekema, Freilassing, Germany) which has a bottom-up lift system. No special slow-cooling protocol was employed during the final sintering step.

At the dentist session, the teeth were clean with air-water spray, dried and an impression was taken from the semi-arch with a polyvinylsiloxane material (Panasil, Kettenbach, Germany). The impression was poured with a high-accuracy polyurethan material (AlphaDie Top, Schütz Dental, Germany) for the production of replicas [7]. After 24 h the replicas were analyzed under a stereomicroscope (STEMI SV6, Zeiss, Germany), sputter-coated and observed in a scanning electron microscope (SEM) (Leitz ISI SR50, Akashi, Japan).

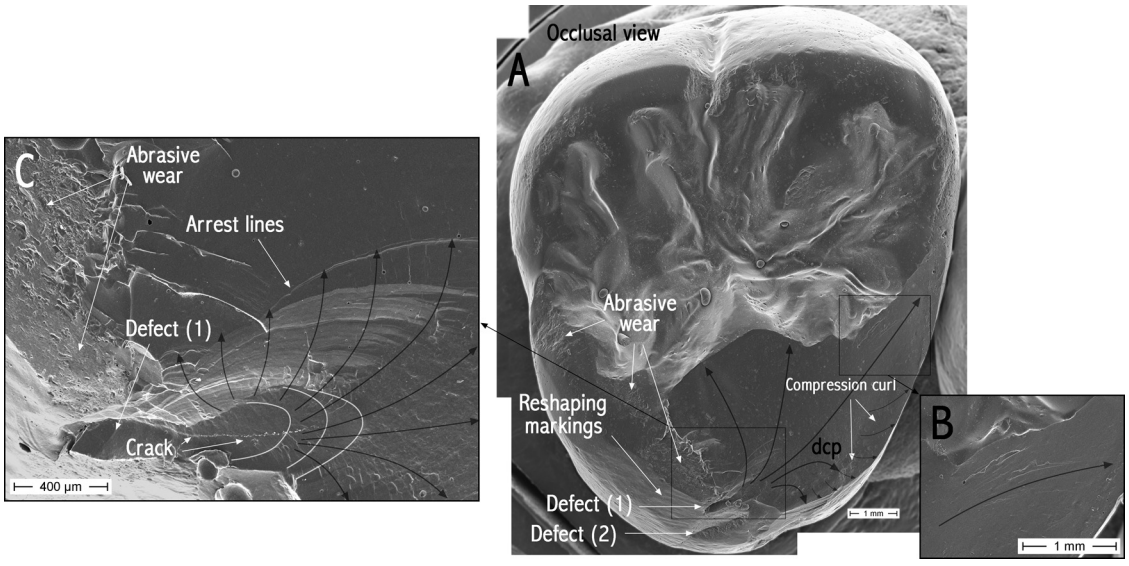

Fig. 2. (A) SEM image of the occlusal view of the fractured crown. Boxes B and C are magnifications. Defect 1 located at the periphery of the occlusal surface and the palatal wall represents the fracture origin (C). Hackle lines (B) indicate that the fracture propagated from the left to the right. Concentric arrest lines on the opposite side reveal that the failure origin is located in the region of the Defect 1. A magnification of this area (C) reveals that the arrest lines are connected to Defect 1, the failure origin. An arrested thin crack can be observed on the base of Defect 1. Nearby this site, reshaping markings and substantial surface damage from abrasive occlusal wear are seen. "dcp" stands for "direction of crack propagation".

2.2. Case 2: 5-unit bridge

The second case deals also with a shell-like fracture of the veneering ceramic of the last abutment tooth (#25) of a ZrO_2-based 5-unit Fixed Dental Prosthesis (FDP) (*i.e.* bridge) that extended from the left first incisor (#21) to the second premolar (#25) (elements #22 and #24 are pontics). Fig. 5 shows the clinical situation of crown #25, where the entire veneering ceramic of the buccal cusp has been lost, along with additional fracture of the ceramic from the buccal surface up to the cervical margin of the restoration.

Retrieval of information from the dentist and the manufacturing laboratory revealed that the FDP consisted of a 3Y-TZP framework (Lava Frame; CTE = 10.5 ppm/°C, 3 M ESPE, Seefeld, Germany) layered with a leucite-based veneering ceramic from the same manufacturer (Lava Ceram) with close matching CTE (10.2 ppm/°C). It had been luted adhesively with a self-adhesive methacrylate-based resin cement (RelyX Unicem, 3M ESPE) on October 1, 2006, having as antagonist a lithium disilicate ceramic crown (e.max CAD, Ivoclar-Vivadent, Liechtenstein) cemented adhesively over a natural tooth abutment. The fracture occurred after 24 months of intra-oral use (Dec. 8, 2008) during normal bite function, as reported by the patient, who recovered the fragment and brought it to the dentist the following day. At that session an impression was taken with a polyvinylsiloxane (Express Penta, 3M ESPE) for the production of replicas (Alpha Die Top) before removal of the entire bridge for replacement. Fragment and replica were analyzed in the light microscope and in the SEM.

3. Fractographic analysis

3.1. Case 1: single crown

The fracture surface provided markings that were used to trace back the fracture origin, from initiation, propagation to the final break off. Wake hackle (Fig. 2) emanating from pores or microstructures of the veneering ceramic are indicative of

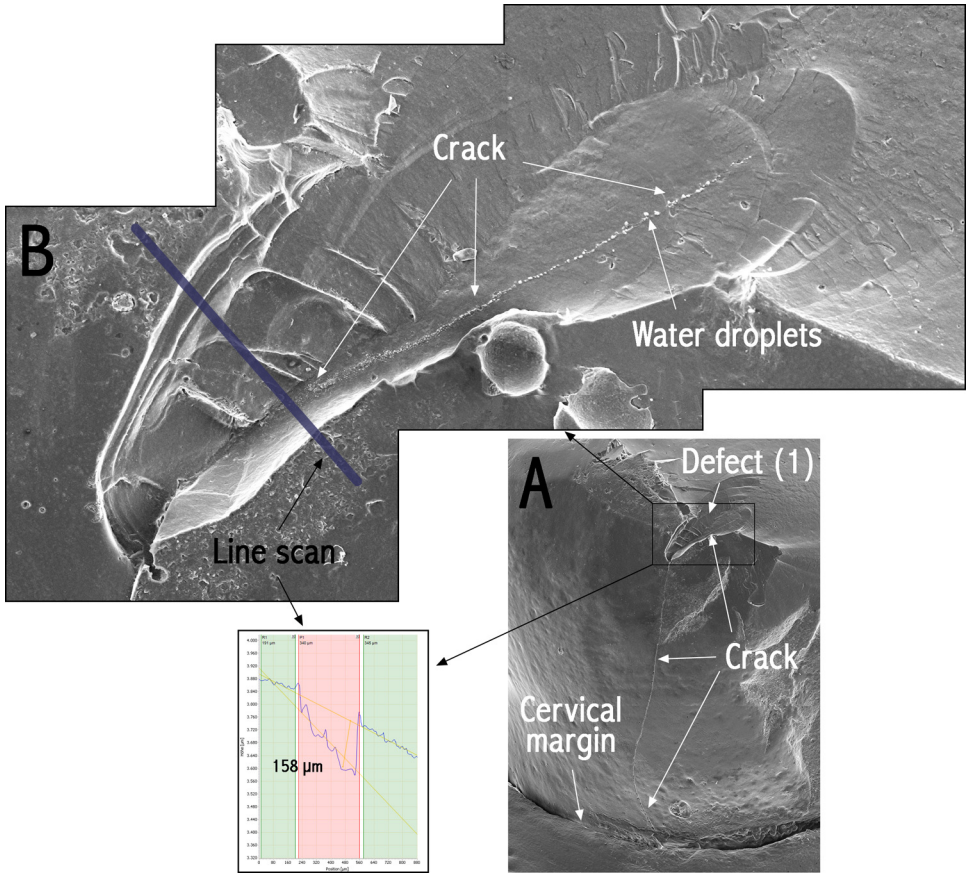

Fig. 3. (A) SEM image of the palatal view of the crown. (B) A magnification of Defect 1 shows that the crack at its base has arrested in the direction of the fracture surface but also propagated in the opposite direction from the edge of Defect 1 towards the cervical margin of the crown. Water droplets emerging from this crack are seen. These droplets could be replicated due to the low polymerization rate of the polyvinylsiloxane impression material. A line scan of the crack origin was made using a optical profilometer and measured to 158 μm in depth.

the direction of crack propagation and were used to locate the origin of the fracture at the midline of the palatal surface where two major surface damages (Defects 1 and 2) were found (Figs. 2 and 3). Working backwards from the occlusal and approximal fracture borders, a zone of concentric arrest lines (Fig. 2) delimitates an elliptical region connected to Defect 1 which was the site of fracture origin. The fracture propagated along the occlusal surface along the black arrows (Fig. 2). A compression curl (*e.g.* a compression lip) visible on the occlusal palato-mesial surface (Fig. 2a) is a result of flexural stress and indicates the end of the fracture event. Adjacent to Defect 1, distinctive signs of contact abrasion can be distinguished, which suggests that the fracture origin was circumscribed within a zone of active occlusal contact loading. A scan of Defect 1 was made using a non-contact white-light optical profilometer (CyberSCAN CT 100, Cyber Technologies, Ingolstadt, Germany) and measured to have a depth of 158 μm (Fig. 3). At the deepest region of Defect 1 a thin crack is observed (Fig. 3), which extended tortuously along the palatal surface (Fig. 4), where it got wider (10 μm) towards the cervical region of the crown. There, a surface scan revealed a 20 μm surface step (unevenness). The presence of fracture markings, pores and microstructural features over the whole fracture surface indicates that no exposure of the ZrO_2 framework had taken place, and a thin layer of the veneering material remained bonded to its surface.

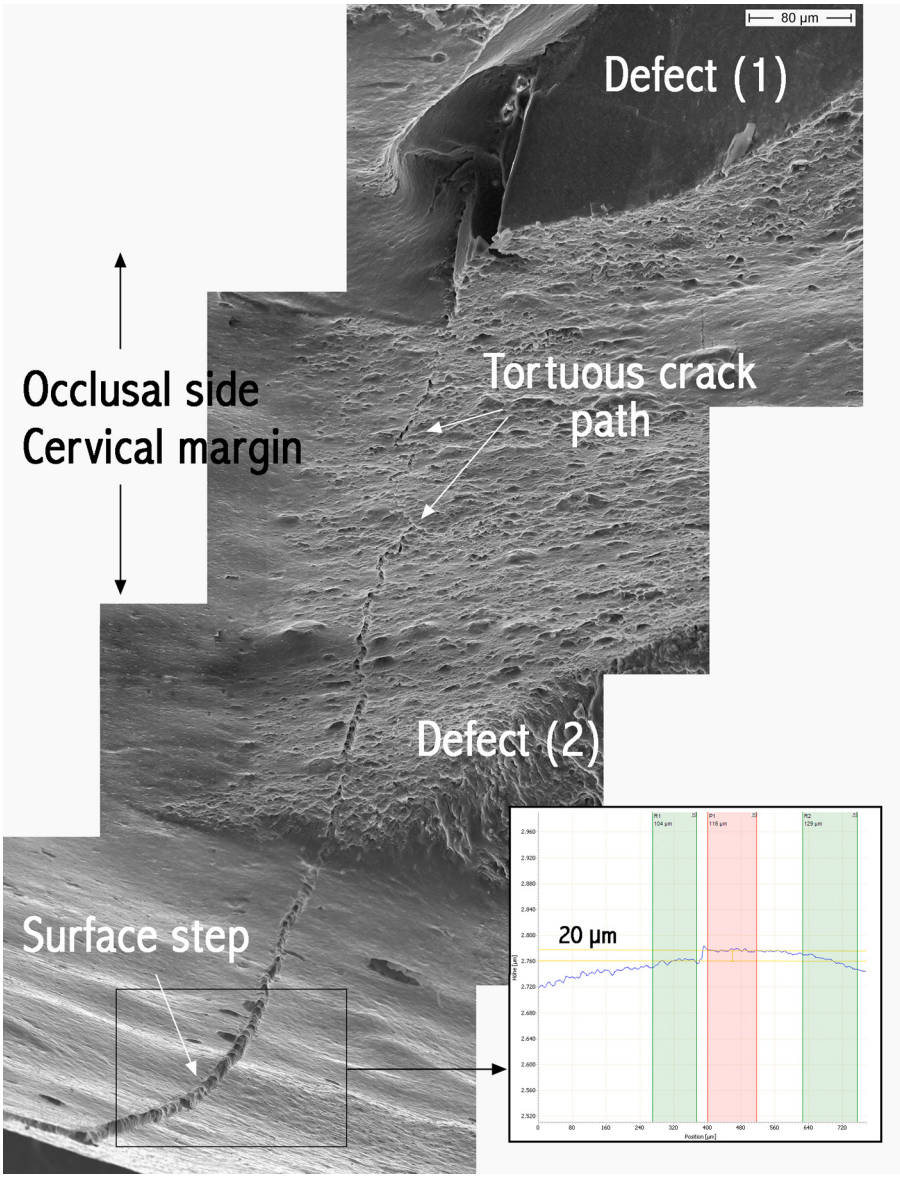

Fig. 4. SEM image of the crack on the palatal surface. The crack connects the origin to the cervical margin. The tortuous crack path suggests that the crack originally grew from inside-out at the palatal side. Towards the cervical margin the crack generates a vertical surface step (unevenness) measured to 20 μm height and a horizontal width opening of 10 μm.

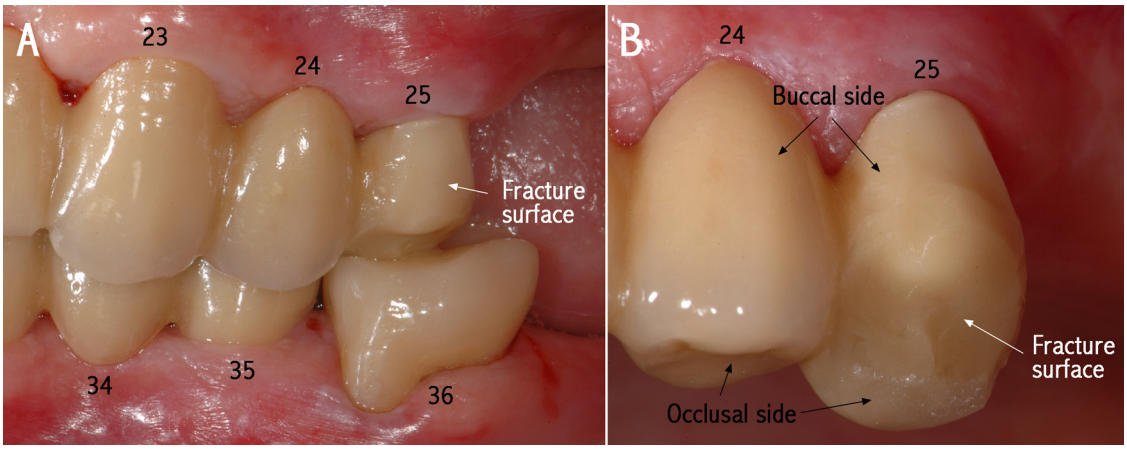

Fig. 5. (A) Buccal view of the clinical condition of Case 2 in occlusion. The fixed prosthesis in the maxilla is a veneered-ZrO_2 5-unit bridge with elements 21, 23 and 25 as abutments, and elements 22 and 24 as pontics (unsupported elements). The fracture occurred in element 25 and involved its buccal cusp and the entire buccal surface reaching the cervical margin. (B) Magnification of elements 24 and 25. The impressions were taken to produce a replica of the fracture surface.

3.2. Case 2: 5-unit bridge (FDP)

The fracture origin was simple to determine from the semi-circular arrest lines that converged to a contact area at the occlusal surface of the recovered fragment (Fig. 6). In this occlusal surface sector a great deal of abrasion is evident (Figs. 7 and 8) showing surface microcracking, with substantial ceramic loss and cracking around the origin (Figs. 7c,d and 8b). Sintering defects were also found on the abraded surface (Fig. 7). At the distal edge of the fragment, partial cone cracks were found on the abraded occlusal surface (Fig. 7), a distinct feature of sliding contact damage. A cross-section of the fragment (not shown) revealed numerous competing cracks extending up to 200 μm from the surface into the bulk of the veneer. The array of arrest lines that developed close to the origin and later after the crack went past the occlusal buccal outer surface of the ZrO_2 framework, could be indicative of fatigue fracture. The arrest lines that developed inwards from the origin point showed a change in orientation (from the normal loading direction) at around ~1.5 mm in depth (arrest lines (1) in Figs. 6

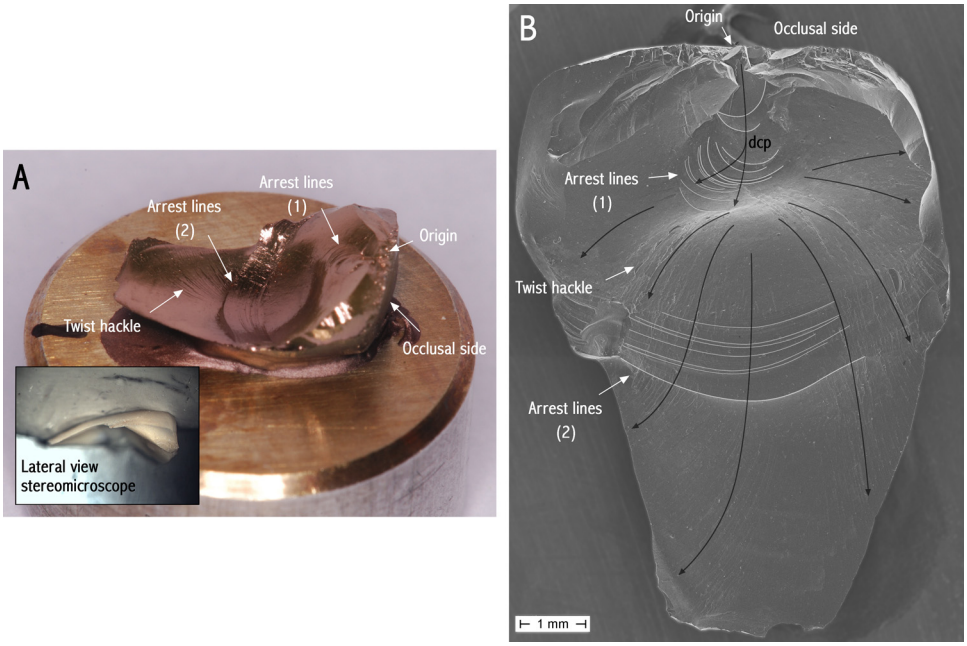

Fig. 6. (A) The recovered fragment was gold-sputtered for SEM analysis. Arrest lines and hackle lines can be distinguished on the fracture surface. Inset shows a lateral view of the fragment under the stereomicroscope before sputtering. (B) SEM image of the fracture surface of the fragment. Two sets of arrest lines are outlined in white. Arrest lines (1) developed under the fracture origin towards the veneering ceramic bulk and show the change in crack orientation due to an oblique loading component. Arrest lines (2) were formed as the crack grew around the convexity of the ZrO_2 framework structure. "dcp" stands for "direction of crack propagation".

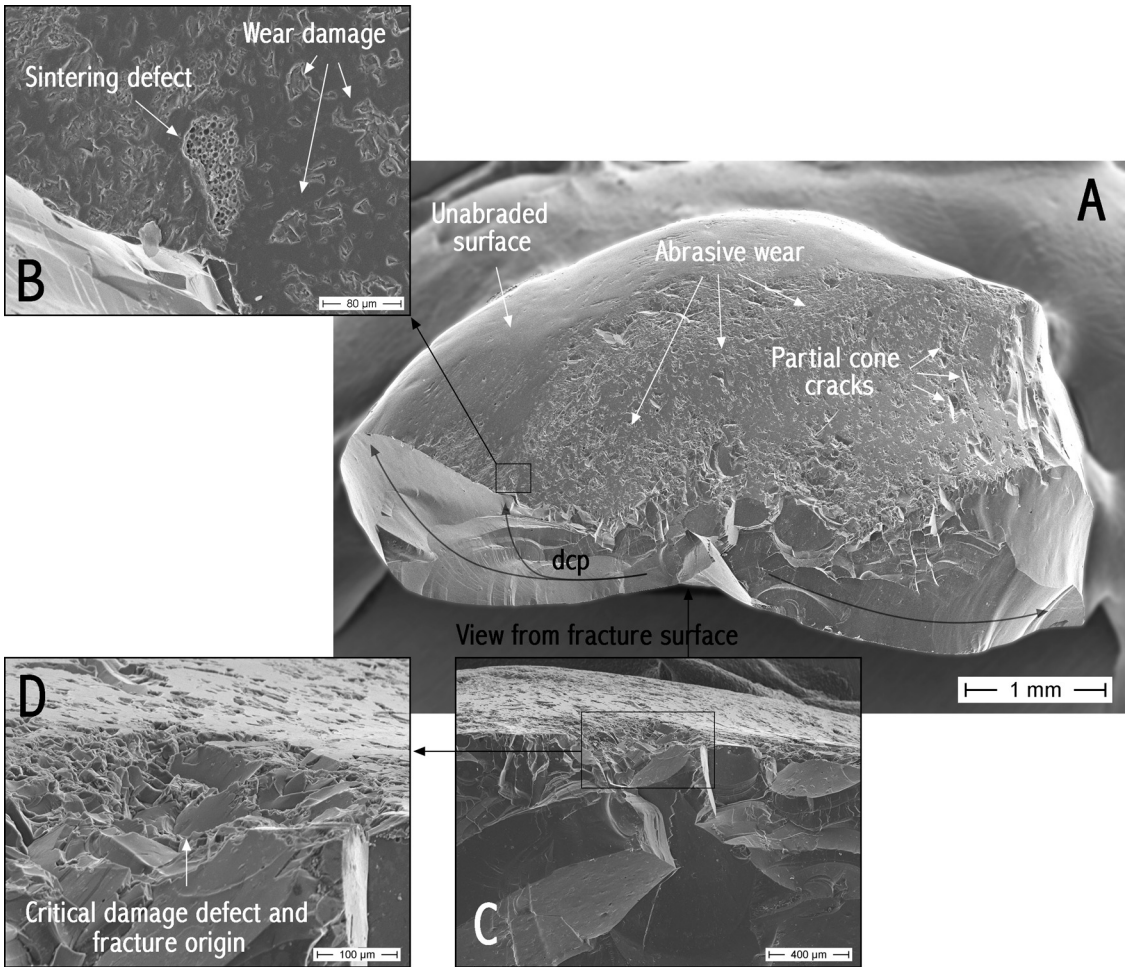

Fig. 7. (A) SEM image of the occlusal view of the veneering ceramic recovered fragment. On the occlusal surface a large area of abrasive contact wear covers the surface. On the right-hand side of the image cracking of the edge and partial cone cracks are visible as part of a contact damage that included sliding and friction. (B) Magnification of an area of the abraded occlusal surface, showing severe wear damage and a sintering defect. (C and D) View from the fracture surface where the fracture origin is located. A large surface contact damage defect is associated with the fracture origin. "dcp" stands for "direction of crack propagation".

and 8a,b), indicating an oblique occlusal loading component. Wake hackle formed from pores often connected subsequent arrest lines (Fig. 8). These markings suggest that a thin layer of the veneering ceramic remained attached to the ZrO_2 surface as seen from the replicated surface (Fig. 8a).

4. Causes of failure and discussion

The prostheses in Cases 1 and 2 are veneered-ZrO_2 systems showing a similar fractographic pattern (shell-like type), although the cause of failure was different for each of them. In Case 1, a veneering material with extremely low CTE was used to cover the ZrO_2 framework, creating a high CTE mismatch of 1.9 ppm/°C. A rough estimation of the residual stresses σ_v that develop in the veneering layer after cooling can be calculated from the general thermal stress equation if a uniform solidification across the veneering ceramic layer is assumed:

$$\sigma_v = \frac{E_v}{1-\nu_v}(\alpha_v - \alpha_i)\Delta T \quad (1)$$

where E_v is the elastic modulus of the veneering ceramic (65 GPa), ν_v its Poisson's ratio (0.21) [8], α_v and α_i the CTEs of respectively the veneering ceramic and the ZrO2 framework, and ΔT is the temperature difference between the glass transition temperature T_g and room temperature (25 °C) for both veneering ceramics: 600 °C for Creation Zi-CT (Case 1) and 565 °C for Lava Ceram (Case 2). The above values of E and ν are typical for dental veneering ceramic materials and were

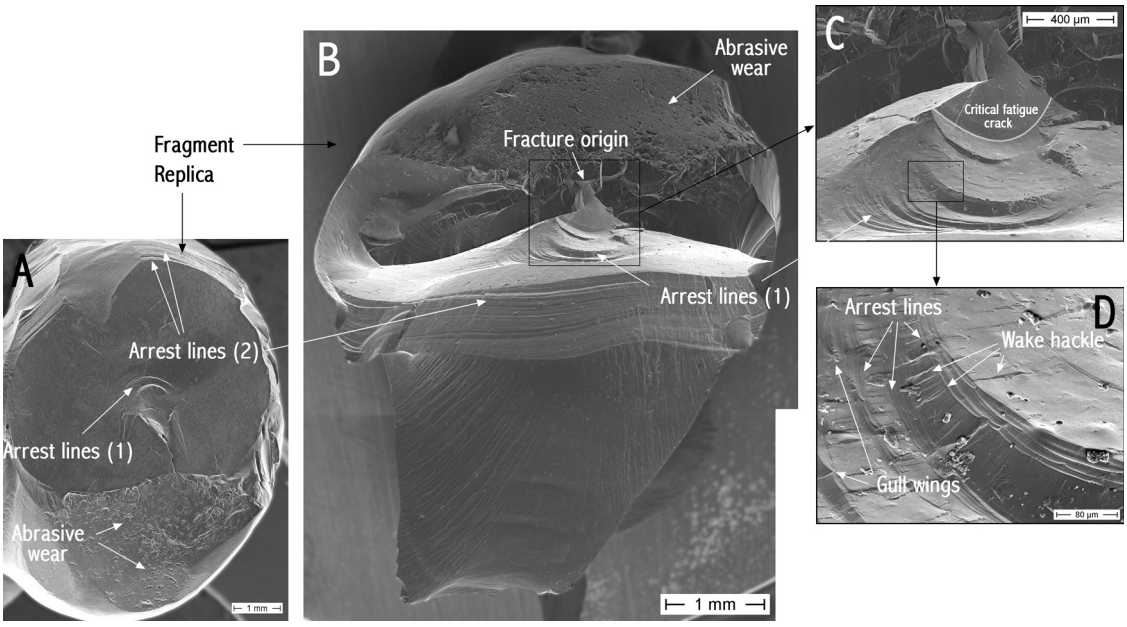

Fig. 8. (A) SEM image of the occlusal side of the replica, showing the two sets of arrest lines that can be matched to the fragment in (B). A substantial area of abrasion is also present on the occlusal surface of the replica. (B) Occlusal and fracture surface view of the fragment. (C and D) Magnifications show the Arrest lines (1) in detail, where wake hackle and other fractographic markings can be seen.

assumed to be the same for both Cases 1 and 2. Values of σ_v give thus −89 MPa and −13 MPa for the veneering ceramic layers in Case 1 and in Case 2, respectively. More accurate solutions for flat geometries that consider thickness ratio, deflections and bending effects can be found elsewhere [9–11], but require values of the curvature of the substrate. Once the cooling across the veneer thickness is not uniform and a great temperature gradient takes place, such compressive stresses are restricted to the interface region, the last region of the veneer to solidify. This zone resists crack propagation and remains attached to the framework, as observed in Cases 1 and 2. Because the sum of stresses in the system must be zero, tensile stresses are generated and redistributed to the framework and to the surface half of the veneering ceramic adjacent to the zone under compression. These tensile stresses are somewhat proportional to the above-calculated values, that is, higher for high CTE mismatch combinations. Fast-cooling (employed for the work in Case 1, but not known for Case 2) just aggravates this scenario [12]. This phenomenon has been observed in a previous study [13] and was implicated in the acceleration of fracture of veneered-ZrO_2 crowns under cyclic contact loading [14], leading also to shell-like fractures *in vitro* [15].

Residual stresses may have accelerated the fracture in Case 1, but the cause of fracture initiation was the deep sharp surface damage (Defect 1) located within an occlusal contact area. The concentration of wear damage around the fracture origin and absent in other regions also point to a possible overloading of the fractured cusp. Using the measured crack size a (158 μm), and the fracture toughness K_c value (~1.0 MPa $\sqrt{m}$ for a typical dental veneering ceramic), the stress at fracture σ_f can be estimated using the basic fracture mechanics relation:

$$\sigma_f = \frac{K_c}{Y\sqrt{a}} \tag{2}$$

where Y is a geometrical factor mainly dependent on the geometry of the crack (here, due to the uncertainty regarding the shape of the initial crack we took an arbitrary value of 1.3, a similar factor for semi-circular surface cracks [16]). σ_f gives 61 MPa, which is lower than the average strength of most dental veneering ceramics (70–100 MPa) [8,17], suggesting the presence of tensile stresses in it. The 20 μm surface step on the palatal surface (Fig. 4) was caused by strain release due to cracking and is a reinforcing indication of the presence of high thermal stresses in the veneer layer in Case 1. It is uncertain if this crack was the primary crack event, but its unusual tortuous path on the palatal side (Fig. 4) suggests that the crack first grew inward from Defect 1 and subsequently outward to the surface (towards the cervical margin). Other aggravating factors such as the implant-supported crown serving as antagonist may have expedited the fracture due to the absence of the damping effect of the natural periodontal ligament.

In Case 2, a pre-existent defect was not identified (although sintering defects were found on the surface), and the critical crack leading to failure was a result of extensive surface contact damage and high contact pressure. On the occlusal surface the wear pattern and the partial cone cracks indicate that severe sliding contact loading took place. This gives rise to a tangential loading component and shear stresses acting at the advancing crack. According to the dentist, the patient

presented severe bruxism habits, a parafunction condition that leads to the patient grinding its teeth for long periods under high muscular tension and pressure forces exercised. Grinding has a large sliding component that creates friction, which magnifies tensile contact stresses. Surface damage was present all over the patient's remaining teeth and prosthetic works. In this Case, the CTE mismatch was low, so no weakening of the veneer material took place, and failure was due to accelerated fatigue contact loading.

5. Conclusions and recommendations

From the analyses of both cases we can conclude that the pre-existent surface defect in association with localized contact overloading and possible thermal residual stresses were found to precipitate the fracture in Case 1, whereas extreme occlusal surface damage from sliding chewing contact was determinant in the fracture of Case 2. From that we can draw some clinical considerations and recommendations:

(1) For veneered-ZrO_2 dental prosthetic restorations, the matching of CTEs is essential in order to minimize detrimental stresses in the veneering ceramic;
(2) Slow-cooling protocols should be employed during the last firing to prevent escalation of thermal stresses;
(3) Before installation, dental prosthetic works should be judiciously inspected under magnification for surface defects created during manufacturing;
(4) Occlusal contacts have to be carefully adjusted intra-orally in order to avoid possible overloading or contacts near the outer periphery from where loss due to chipping of the veneering ceramic can easily occur;
(5) Despite the high-strength ZrO_2 framework, the brittle overlaying glass–ceramic is subject to surface damage when exposed to contact loads. Extreme loading scenarios will accelerate surface damage and failure of the material;
(6) Bruxism should be considered as a contra-indication for veneered all-ceramic fixed dental prostheses.

References

[1] Al-Amleh B, Lyons K, Swain M. Clinical trials in zirconia: a systematic review. J Oral Rehabil 2010;37:641–52.
[2] Raigrodski AJ, Chiche GJ, Potiket N, Hochstedler JL, Mohamed SE, Billiot S, et al. The efficacy of posterior three-unit zirconium-oxide-based ceramic fixed partial dental prostheses: a prospective clinical pilot study. J Prosthet Dent 2006;96:237–44.
[3] Sailer I, Feher A, Filser F, Gauckler LJ, Luthy H, Hammerle CH. Five-year clinical results of zirconia frameworks for posterior fixed partial dentures. Int J Prosthodont 2007;20:383–8.
[4] Heintze SD, Rousson V. Survival of zirconia- and metal-supported fixed dental prostheses: a systematic review. Int J Prosthodont 2010;23:493–502.
[5] Sailer I, Gottnerb J, Kanelb S, Hammerle CH. Randomized controlled clinical trial of zirconia–ceramic and metal–ceramic posterior fixed dental prostheses: a 3-year follow-up. Int J Prosthodont 2009;22:553–60.
[6] Benetti P, Kelly JR, Della Bona A. Analysis of thermal distributions in veneered zirconia and metal restorations during firing. Dent Mater 2013;29:1166–72.
[7] Scherrer SS, Quinn JB, Quinn GD, Wiskott HW. Fractographic ceramic failure analysis using the replica technique. Dent Mater 2007;23:1397–404.
[8] Borba M, de Araújo MD, Fukushima KA, Yoshimura HN, Cesar PF, Griggs JA, et al. Effect of microstructure on the lifetime of dental ceramics. Dent Mater 2011;27:710–21.
[9] Freund LB, Suresh S. Thin film materials: stress, defect formation and surface evolution. UK: University of Cambridge Press; 2003.
[10] Freund LB. Substrate curvature due to thin film mismatch strain in the nonlinear deformation range. J Mech Phys Solids 2000;48:1159–74.
[11] Hsueh C-H. Modeling of elastic deformation of multilayers due to residual stresses and external bending. J Appl Phys 2002;91:9652–6.
[12] Swain MV. Unstable cracking (chipping) of veneering porcelain on all-ceramic dental crowns and fixed partial dentures. Acta Biomater 2009;5:1668–77.
[13] Belli R, Monteiro Jr , Baratieri LN, Katte H, Petschelt A, Lohbauer U. A photoelastic assessment of residual stresses in zirconia-veneer crowns. J Dent Res 2012;91:316–20.
[14] Belli R, Frankenberger R, Appelt A, Schmitt J, Baratieri LN, Greil P, et al. Thermal-induced residual stresses affect the lifetime of zirconia-veneer crowns. Dent Mater 2013;29:181–90.
[15] Belli R, Petschelt A, Lohbauer U. Thermal-induced residual stresses affect the fractographic patterns of zirconia-veneer dental prostheses. J Mech Behav Biomed Mater 2013;21:167–77.
[16] Mecholsky Jr . Fracture mechanics principles. Dent Mater 1995;11:111–2.
[17] Gonzaga CC, Cesar PF, Miranda Jr , Yoshimura HN. Slow crack growth and reliability of dental ceramics. Dent Mater 2011;27:394–406.